A Supercritical Pressure Parallel Channel Natural Circulation Loop

Manish Sharma, Kapil Bodkha, D.S. Pilkhwal and P.K. Vijayan
Bhabha Atomic Research Centre, Trombay, Mumbai, India

Abstarct: Supercritical water is being considered as a coolant in some advanced nuclear reactor designs on account of its potential to offer high thermal efficiency, compact size, elimination of steam generator, separator & dryer. As the nuclear reactor core comprises of many parallel channels, understanding supercritical flow stability in parallel channels would be important for reactor design and licensing. A closed Supercritical Pressure Parallel Channel Loop (SP-PCL) based on natural circulation with water as working fluid is proposed to be built in Bhabha Atomic Research Centre (BARC), India. A computer code NOLSTA-p has been developed to carry out steady state and stability analysis of SP-PCL. Code predicts a very large unstable zone for SP-PCL without considering pipe wall thermal capacitance effect. However, the loop becomes completely stable on incorporating pipe wall thermal capacitance model in the computer code. The details of SPNCL, its modeling and analysis are presented in this paper.

1. Introduction

Supercritical water is being considered as a coolant in some advanced nuclear reactor designs on account of its potential to offer high thermal efficiency, compact size, elimination of steam generator, separator & dryer, making it economically competitive. The elimination of phase change results in elimination of the CHF phenomenon. Supercritical water natural circulation loops are capable of generating density gradients comparable to two-phase natural circulation loops. Hence, Supercritical water under natural circulation is also considered as a viable option of heat removal in supercritical water cooled reactors, Silin et al. (1993) and Bushby et al. (2000). Safety is a key issue in the design of advanced reactors and considerable emphasis is placed on passive safety. Cooling a reactor at full power with natural instead of forced circulation is generally considered as enhancement of passive safety. Hence, the behaviour of steady state natural circulation with supercritical fluids is of interest for a number of new reactor systems. Besides stable steady state, operation with unstable natural circulation is undesirable as it can lead to power oscillations in natural circulation based supercritical water reactors. Moreover, it can also cause mechanical vibration of components and failure of control systems. Since supercritical water (SCW) or any other supercritical fluid experiences steep change in its thermo-physical properties (e.g. density) near the pseudo-critical temperature, supercritical water reactors may be susceptible to density wave instability. As the nuclear reactor core comprises of many parallel channels, understanding supercritical flow stability in parallel channels would be important for reactor design and licensing. When flow instability occurs between parallel multi-channels, the mass flow of each channel fluctuates periodically, while total mass flow of parallel multi-channels is stable.

Several researchers have investigated theoretically the stability in supercritical fluid natural circulation loops with single heated channels i.e. Chatoorgoon (2001), Jain and Corrrandini (2006), Ambrosini and Sharabi (2008), Chatoorgoon et al.(2005), Jain and Rizwan-uddin, (2008), Chen et al. (2010) etc. Few researchers have also studied supercritical flow instability for parallel heated channels. Hou et al. (2011) did a linear and non-linear analysis of parallel channel within the Supercritical Water Reactor (SCWR) core and compared the results. Xi et al. (2014) did a three dimensional (3D) numerical simulation is carried out using the CFX code to investigate the out of phase oscillation between two heated parallel channels with supercritical water. Finally, the numerical result is compared with experimental data of Xiong et al. (2012). Su et al. (2013) analyzed the flow instability of SCW using the tiny perturbation method. The effects of different parameters, such as mass flow rate, heat flux, inlet temperature and system pressure, on the flow instability boundary were investigated. They concluded that increasing the mass flow rate and the system pressure, decreasing the heat flux, the flow stability in the parallel channels increases.

The literature reveals only very few experimental studies on natural circulation with supercritical fluids and most of them are for single channels. Harden and Boggs et al. (1964) conducted studies on Freon loops near critical region. High and low frequency oscillations were observed when bulk fluid temperature approached pseudo-critical temperature. Adelt and Mikielewicz (1981) performed studies on 4m high loop with carbon-dioxide (CO_2). As the fluid was heated through pseudo-critical point pressure oscillations were observed for a particular test but the study mainly focused upon heat transfer rather than stability. Lomperski et al. (2004) have reported experiments in a two meter high natural circulation loop with carbon-dioxide at supercritical pressure. The loop was operated in a base case configuration that maximized flow rates and in

a second configuration having an orifice in the hot leg. No flow instabilities were observed in these tests as the fluid was heated through thermodynamic pseudo-critical point. Yoshikawa et al. (2005) have studied the performance of a natural circulation system for supercritical CO_2. In a very recent study, T'Joen and Rhode (2012) conducted stability experiments with artificial neutronic feedback in scaled natural circulation driven HPLWR (High Performance Light Water Reactor) facility named Delight maintaining the inlet temperature constant (i.e. with open loop boundary conditions). They used Freon R23 at 5.7 MPa as the scaling fluid. The decay ratios and frequencies of the riser inlet temperature oscillations were measured. They found that for a single inlet temperature the system undergoes two transitions as the power is increased. At low power the system is stable and becomes unstable as the power is increased, but on further increasing the power the system stabilizes. They also found a threshold inlet temperature above which no instability is observed. Steady state and stability experiments have been reported for closed Supercritical Pressure Natural Circulation Loop (SPNCL) with two different operating fluids i.e. supercritical carbon-dioxide; Sharma et al. (2013) and supercritical water; Sharma et al. (2014).

A few experiments have also been reported for parallel channels. Xiong et al. (2012) have reported experimental data on flow instability in two parallel channels with supercritical water. Experimental conditions included pressures of 23–25 MPa, mass fluxes of 600–800 kg/m^2 s, and inlet temperatures of 180–260 °C. Parametric studies show that the flow becomes more stable with increasing pressure or decreasing inlet temperature in the range of present experiments. Out of phase flow instability between two heated channels with supercritical water was observed by Xi et al.(2014) in his experimental investigation.

The Supercritical Pressure Natural Circulation Loop (SPNCL) having single heated channel was operated at Bhabha Atomic Research Centre (BARC), India. The same loop is proposed to be modified for studying the effect of two parallel heated channels. A computer code NOLSTA, described in Sharma et al., 2013 has been modified for studying the steady state and stability behavior of parallel channel systems.

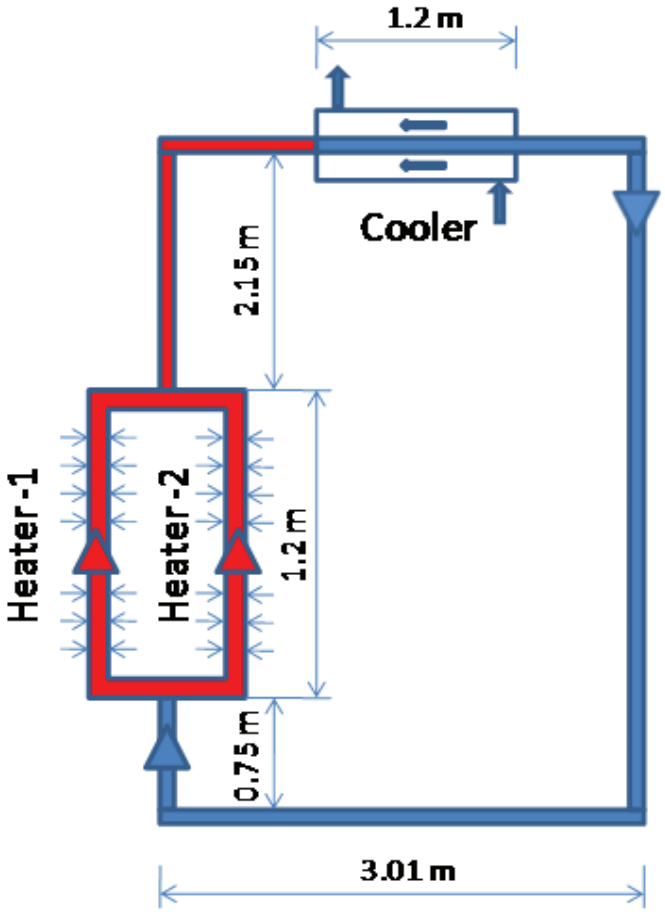

Figure 1: Schematic of SP-PCL

2. The proposed loop

The proposed loop is a uniform diameter pipe (13.88 mm ID & 21.34 mm OD). It is a rectangular Supercritical Pressure Parallel Channel Loop (SP-PCL) based on natural circulation with a schematic shown in Figure 1. The loop has two vertical parallel channel heaters and a top horizontal cooler. The cooler is tube in tube type with supercritical water flowing in the inner tube and air flowing in the outer annular tube (38.14 mm ID).

3. NOLSTA-p Code Development

The **NO**n-**L**inear **ST**ability **A**nalysis – **p**arallel (NOLSTA-p) code has been developed for analyzing stability of natural circulation loops operating with two parallel heated channels. The code solves the mass, momentum and energy equations by applying time domain approach. Steady state solutions are obtained. A small perturbation is imposed on the steady state results to get the dynamic response of the system. If amplitude of perturbation increases with time the flow is unstable and if the amplitude of perturbation dies out with time the flow is stable. If the amplitude of the perturbation remains same with time the flow is neutrally stable and the corresponding heater power is the threshold of instability.

3.1 Open Loop

In an open loop the fluid temperature at the inlet of the two heaters is fixed irrespective of the heater power. The heat that is added in two heaters is rejected in cooler there by maintaining heaters inlet temperature constant.
In this case, the operating pressure of the loop, inlet fluid temperature to the heaters and the heaters powers are specified along with the entire geometry of the loop (hydraulic diameter, flow area and length of each pipe).

3.1.1 Governing equations
In one dimensional analysis the only co-ordinate x, runs around the loop with origin at the outlet of cooler. The governing continuity, momentum and energy equations for one dimensional flow can be written as,
Continuity:

$$A\frac{\partial \rho}{\partial t}+\frac{\partial w}{\partial x}=0 \tag{1}$$

Momentum:

$$\frac{\partial w}{\partial t}+\frac{\partial}{\partial x}\left(\frac{w^2}{\rho A}\right)+A\frac{\partial p}{\partial x}+\left(\frac{f}{D}+K\right)\frac{w^2}{2\rho A}+\rho A g\cos\phi=0 \tag{2}$$

Energy:

$$A\frac{\partial(\rho i)}{\partial t}+\frac{\partial(wi)}{\partial x}+wg\cos\phi=q'''A+A\frac{\partial p}{\partial t} \tag{3}$$

In addition an equation of state is required for the density and is given by

$$\rho = f(p,i) \tag{4}$$

Supercritical water properties were approximated from data tables obtained from National Institute of Standards and Technology(NIST) database (http://webbook.nist.gov/chemistry/fluid/).The equations remain same for both the channels as well as for rest of the loop, except that the equations are applied individually to each heater channel by assuming a flow rate distribution at inlet of two channels. The mass flow rate distribution converges when outlet pressure of each channel becomes equal. The set of mass, momentum and energy conservation equations is closed by equation of state for the supercritical fluid. The steady state solution can be obtained by dropping the time derivatives from the above equations. These are

$$\frac{\partial w}{\partial x} = 0 \tag{5}$$

$$\frac{\partial}{\partial x}\left(\frac{w^2}{\rho A}\right) + A\frac{\partial p}{\partial x} + \left(\frac{f}{D} + K\right)\frac{w^2}{2\rho A} + \rho A g \cos\phi = 0 \tag{6}$$

$$\frac{\partial (wi)}{\partial x} + wg\cos\phi = \begin{cases} q_h''' \text{ A or } -q_c''' \text{A} & \textit{for heater or cooler region,} \\ 0 & \textit{adiabatic region.} \end{cases} \tag{7}$$

Control volume discretization in space using upwind scheme is employed to derive the difference equations for mass, momentum and energy conservation. In deriving the difference equations, the effect of integrating across a computational cell is analogous to averaging the field variables in that section and leads to better accuracy compared to first order difference schemes for the spatial derivatives (Dogan et al., 1983).

3.1.2 Discretization of governing equations for steady state solution

Integrating the steady state mass, momentum and energy equations (5,6 and 7) across the control volume from j to j+1, where j & j+1 are grid points at inlet and outlet face of the control volume, leads to following set of discretized equations:

Continuity:

$$w_{j+1} = w_j \tag{8}$$

Momentum:

$$p_{j+1} = p_j - \left(1 + \frac{1}{4}\left(\frac{f}{D}\Delta x + K\right)\right)\left(\frac{w^2}{\rho A^2}\right)_{j+1} + \left(1 - \frac{1}{4}\left(\frac{f}{D}\Delta x + K\right)\right)\left(\frac{w^2}{\rho A^2}\right)_j - \left(\frac{\rho_j + \rho_{j+1}}{2}\right) g\,\Delta z \tag{9}$$

Energy:

$$i_{j+1} = i_j - g\Delta z + \frac{(q_h''' or - q_c''')A\,\Delta x}{w_j} \qquad \text{for heater or cooler} \tag{10}$$

$$\rho_{j+1} = f(p_{j+1}, i_{j+1}) \tag{11}$$

Boundary conditions:
(i) For open loop fluid temperature at inlet of heater is fixed and whatever heat is added in two heaters is rejected in cooler there by maintaining heater inlet temperature constant.
(ii) The pressure at the first control volume should be equal to the pressure calculated by equation (9) for the last control volume (i.e. $\Sigma\Delta p = 0$).
(iii) Inlet pressures to the two heater channels is equal to the outlet pressure of the last control volume just before the two parallel channels control volumes start.
(iv) The outlet pressure of the last control volumes of each of the two parallel channels should be equal and this is achieved by distributing mass flow rate at inlet of two parallel channels such that outlet pressure becomes equal, as calculated by equation 9.

While the density at any axial distance is known from equation (11), the friction factor in the single-phase region (sub-critical or supercritical), is obtained from the local Reynolds number as follows.

$$f_{la\,\min ar} = 64/\mathrm{Re} \qquad \text{as given by Poiseuille's law for laminar flow} \tag{12}$$

$f_{turbulent} = 0.316 / \mathrm{Re}^{0.25}$ as given by Blasius correlation for turbulent flow (13)

and friction factor used in the calculations is selected as the maximum value calculated by the above two equations, i.e.

f = maximum of ($f_{laminar}$, $f_{turbulent}$) (14)

This has been done to avoid discontinuity in the friction factor value during transition from laminar to turbulent flow. There are several correlations available in literature for calculation of friction factor for turbulent supercritical flows; however no single correlation is applicable under all operating conditions. Hence, to start with Blasius correlation is considered for simulation of pressure drop at supercritical conditions.

3.1.3 Discretization for time dependent solution
Integrating time dependent conservation equations (1), (2) & (3) across the control volume from j to j+1 leads to following set of discretized equations:
Continuity:

$$(w)_{j+1}^{n+1} = (w)_{j}^{n+1} - \left(\rho_{j+1}^{n+1} - \rho_{j+1}^{n} + \rho_{j}^{n+1} - \rho_{j}^{n}\right)\frac{A\Delta x}{2\,\Delta t} \tag{15}$$

Momentum:

$$p_{j+1}^{n+1} = p_{j}^{n+1} - \left(1 + \frac{1}{4}\left(\frac{f}{D}\Delta x + K\right)\right)\left(\frac{w^2}{\rho A^2}\right)_{j+1}^{n} + \left(1 - \frac{1}{4}\left(\frac{f}{D}\Delta x + K\right)\right)\left(\frac{w^2}{\rho A^2}\right)_{j}^{n} - \left(\frac{\rho_{j}^{n} + \rho_{j+1}^{n}}{2}\right) g\,\Delta z$$
$$- \left((w)_{j+1}^{n+1} - (w)_{j+1}^{n} + (w)_{j}^{n+1} - (w)_{j}^{n}\right)\frac{\Delta x}{2\,A\Delta t} \tag{16}$$

Energy:

$$i_{j+1}^{n+1}\left((w)_{j+1}^{n+1} + \frac{A\Delta x}{2\,\Delta t}\rho_{j+1}^{n+1}\right) - i_{j}^{n+1}(w)_{j}^{n+1} + \left((w)_{j+1}^{n+1} + (w)_{j}^{n+1}\right)g\frac{\Delta z}{2} + T$$
$$= q''' A\Delta x + \frac{A\Delta x}{2\,\Delta t}\left(p_{j+1}^{n+1} + p_{j}^{n+1} - p_{j+1}^{n} - p_{j}^{n}\right) \tag{17}$$

where

$$T = \frac{A\Delta x}{2\Delta t}(\rho i)_{j}^{n+1} - \frac{A\Delta x}{2\Delta t}\left[(\rho i)_{j+1}^{n} + (\rho i)_{j}^{n}\right] \tag{18}$$

4. Analysis

4.1 Qualitative assessment of NOLSTA-p code

NOLSTA-p code has been validated for open loop analysis with experimental data generated by Xiong et al. (2012) for parallel channel with forced circulation. The simplified geometrical model proposed by Xiong et al. for their experimental loop is shown in figure 2. The model consists of two parallel channels connected at bottom with common lower plenum and at top with common upper plenum. The heights of the entrance and riser sections for each channel are 200 mm and 350 mm respectively. The two heated sections for each channel have inner and outer diameter of 6 mm and 11 mm, while the heated length is 3000 mm each.

The inlet/ outlet pressure drop coefficients suggested by Xiong et al. based on simplification of his experimental loop exhibit certain differences between two channels as represented in figure 2 by orifices at inlet and outlet of each channel i.e.
For channel-1, $K_{in,1} = 5.4$, $K_{out,1} = 4.93$ and for channel-2, $K_{in,2} = 5.5$, $K_{out,2} = 6.46$
The boundary conditions are as follows

i) Total mass flow rate, temperatures and pressures at inlet of two parallel channels is constant.
ii) Pressures at outlet of two parallel channels should be equal, i.e., $P_{out,1} = P_{out,2}$

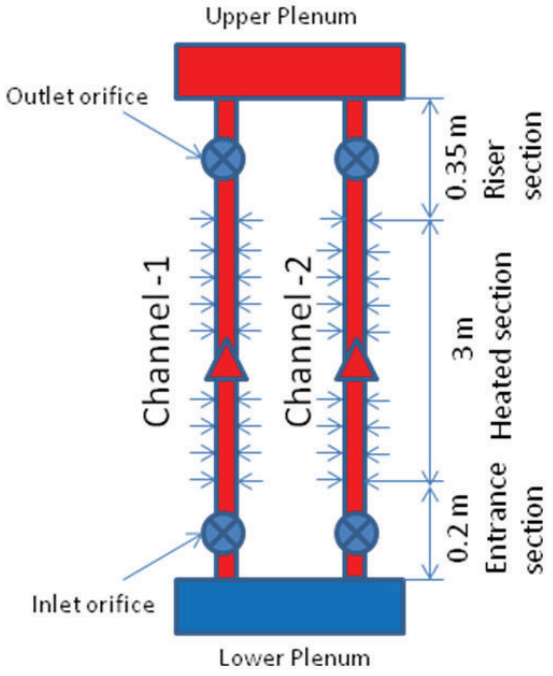

Figure 2: Proposed geometrical model corresponding to experimental loop of Xiong et al. (2012)

Considering above boundary conditions the threshold power of instability is predicted using NOLSTA-p code for different inlet temperatures. The instability prediction requires first calculation of steady state mass flow rates for individual channels for given powers which is taken as an initial condition for transient predictions of mass flow rates for each channel. The transient predictions have been made for inlet conditions of 250 bar, 220 ^{o}C and total inlet flow rate of 120 kg/h. If the amplitudes of the mass flow rate oscillations decrease with time, it is a stable case as shown in figure 3a for 31 kW. If the amplitudes of the mass flow rate oscillations increase with time, it is an unstable case as shown in figure 3b for 32 kW. If the amplitudes of the mass flow rate oscillations remain same with time, it is a neutrally stable case as shown in figure 3c for 31.2 kW. So 31.2 kW is considered as the predicted threshold power of instability. The oscillations in the two channels are out of phase as is evident from figure 3a, 3b and 3c.

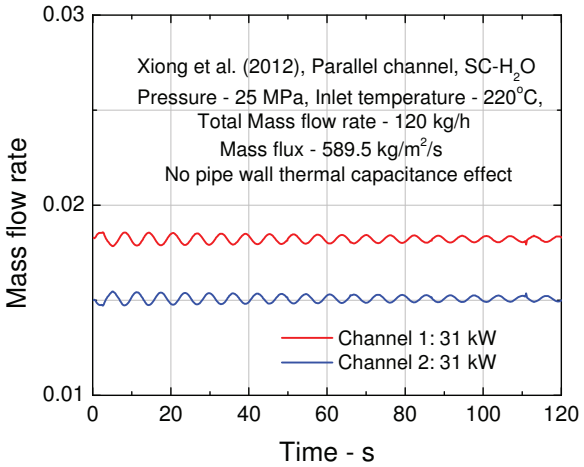

3a: Stable

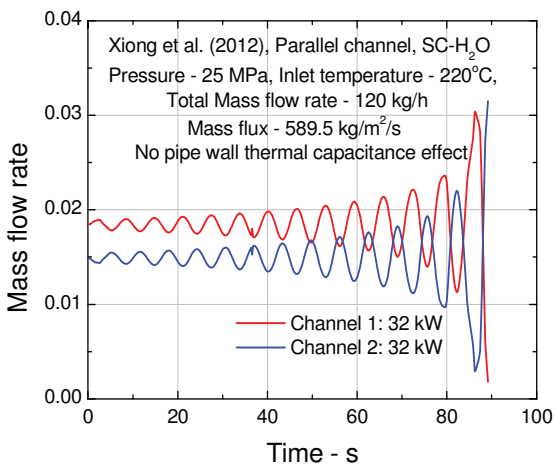

3b: Unstable

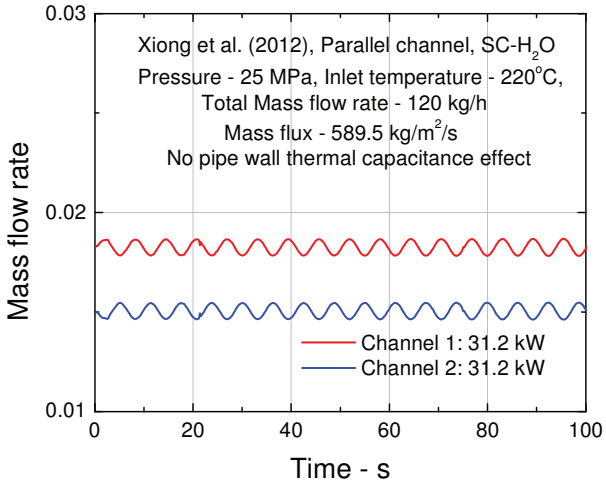

3c: Neutrally stable

Figure 3: Threshold of instability predicted by NOLSTA-p code

The threshold power of instability was also predicted for different inlet temperature conditions (i.e. 200 °C & 240 °C) to compare with the experimental threshold powers of instability reported by Xiong et al. (2012). The predicted threshold powers of instability have a maximum deviation of 9.4% from experimental threshold power values as shown in figure 4. However beyond 240 °C the experimental threshold power of instability could not be determined as maximum allowable heater wall temperature was exceeded.

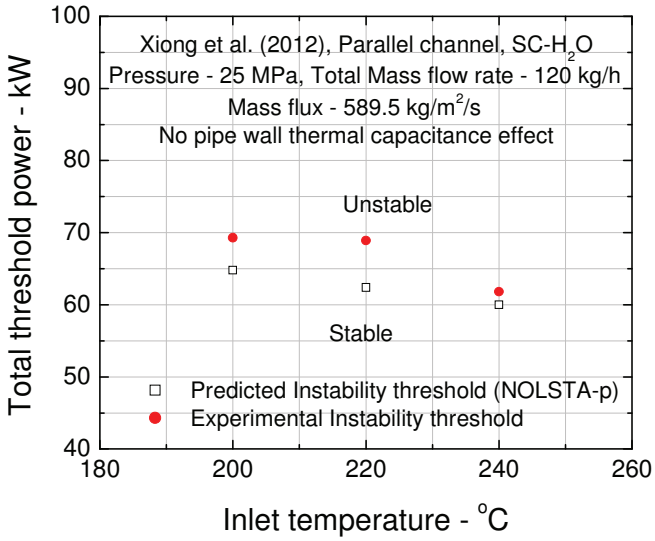

Figure 4: Comparison of predicted instability threshold with experimental threshold reported by Xiong et al. (2012)

4.2 Steady state analysis of Closed Loop SP-PCL

The proposed SP-PCL is actually a closed loop where inlet temperature to heaters is not controlled and only air mass flow rate and inlet temperature on secondary side of cooler is maintained constant. The heater inlet temperature is not fixed and increases with increase in power of both the heaters. For analysis of closed loop, the rate of heat rejection in the cooler is evaluated based on calculation of overall heat transfer coefficient for cooler and temperature difference between primary and secondary fluid as described in Sharma et al. (2013). In this case, the operating pressure of the loop, coolant mass flow rate & inlet

temperature for secondary side of cooler and the power of both the heaters are specified along with the entire geometry of the loop (hydraulic diameter, flow area and length of each pipe).

. The governing equations for its analysis remain same as given in section 3.1.1, 3.1.2 & 3.1.3. The procedure to achieve steady state mass flow rate is explained below:

(i) Assume an inlet temperature to the two heaters and calculate the steady state mass flow rate of SP-PCL for a given total power by assuming total heat rejection in cooler or considering open loop configuration.
(ii) Now taking this flow rate and temperature distribution on primary side of cooler evaluate UA_h x LMTD for cooler.
(iii) If UA_h x LMTD < Power given to heaters then increase inlet temperature of the heaters else reduce inlet temperature of the heaters. The iterations converge if UA_h x LMTD is within 99.9% of the power given to heaters.

The steady state mass flow rate variation of SP-PCL with respect to power of channel-1 and different power ratios of channel-2 to channel-1 (P_2/P_1=1.0, 0.5 and 0.01) is shown in figure 5. For all the power ratios, the total mass flow rate as well as individual channel mass flow rate increases till total power reaches approximately 8 kW due to increase of buoyancy force and after that the mass flow rates start reducing due to increased frictional resistance.

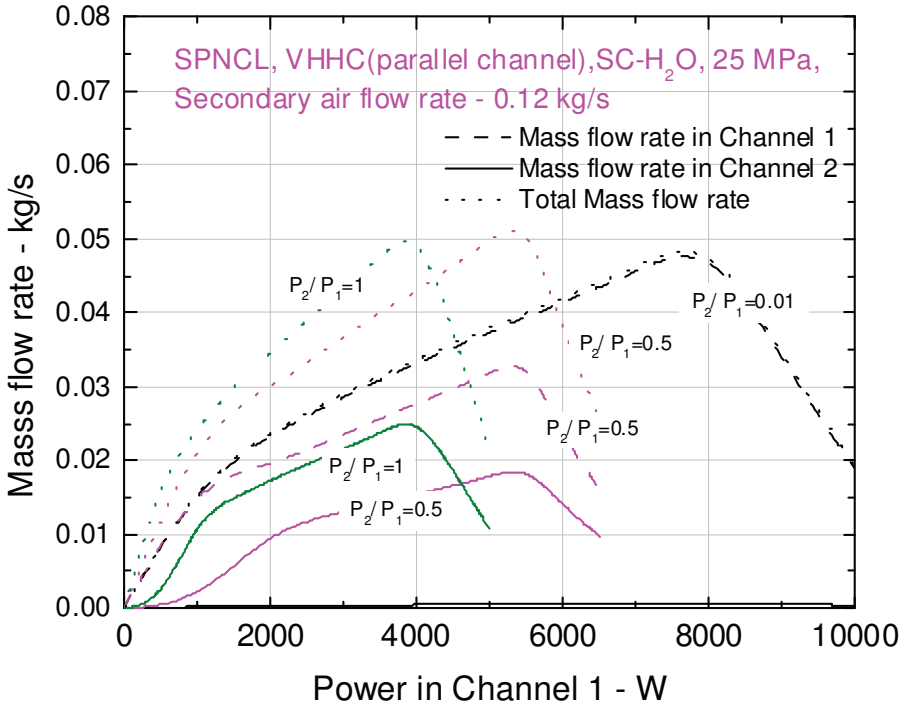

Figure 5: Steady state characteristic of SP-PCL

The variation of steady state mass flow rate for constant power (2500 W) in channel-1 and varying power in channel-2 is shown in figure 6. The mass flow rate of constant power channel keeps reducing as the power in other channel increases. However, mass flow rate in channel-2 and the total mass flow rate keeps increasing till total power of two channels reach 8 kW and the mass flow rates start reducing when power increases beyond 8 kW. Figure 6 also shows the effect of pressure on steady state flow rate which remains almost same for different pressures i.e. 22.5 MPa and 25 MPa in the buoyancy dominant regime up to 8 kW however in friction dominant regime mass flow rate is lower at lesser pressure i.e. 22.5 MPa. This is because of lower density and higher frictional resistance at lower pressures.

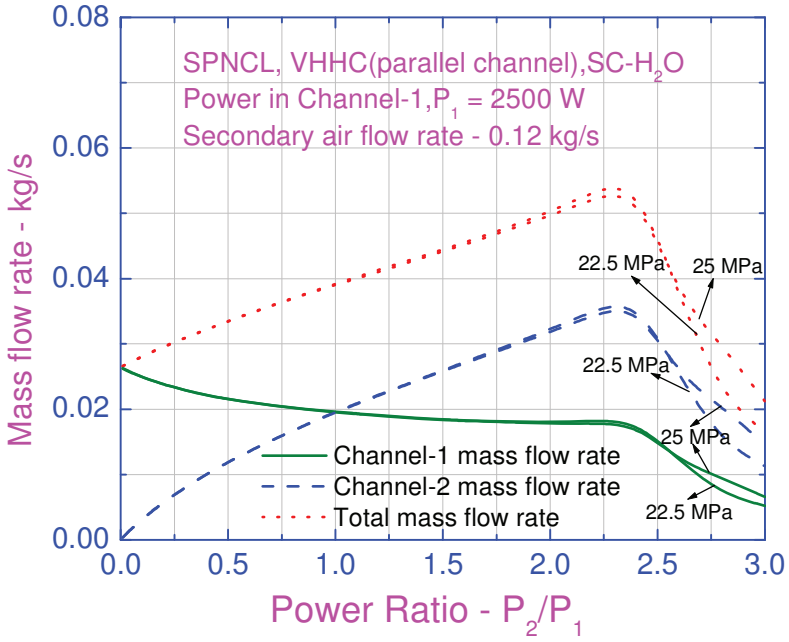

Figure 6: Effect of pressure on steady state flow rate of SP-PCL

4.3 Stability analysis of closed loop SP-PCL

4.3.1 Sensitivity study

The stability analysis was carried out for SP-PCL considering closed loop behaviour in which pipe wall thermal capacitance is not considered. The stability threshold for closed loop boundary conditions has been found to be sensitive to the time step and grid size used for analysis; hence a time step and grid size independence test was carried out.

4.3.1.1 Effect of time step and grid size

To start with grid size of 0.05 m was considered and time steps were changed to carry out the stability analysis of SP-PCL at 2000 W (1000 W in each heater channel)/ 22.5 MPa. It was observed that larger time steps stabilized the predictions as shown in figure 7. On reducing the time step from 0.06 s to 0.03 s the predictions hardly change. Now considering 0.06 as the time step the grid size was reduced to 0.025 m but no change was observed in the results as shown in figure 8. To preserve accuracy and save computational time the grid size of 0.05 m was finalized. Henceforth, grid size and time step of 0.05 m and 0.06 s respectively have been used for generating the stability results for SP-PCL with closed loop boundary conditions.

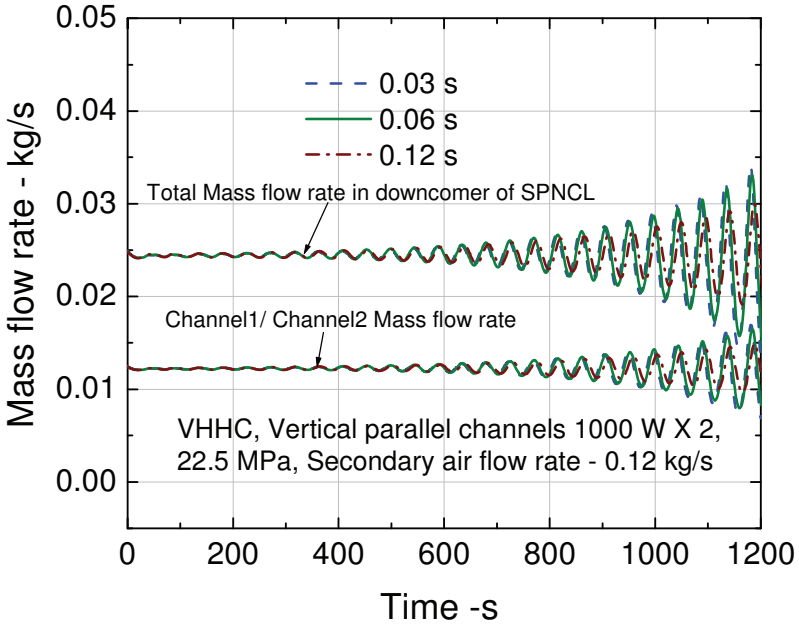

Figure 7: Time step sensitivity study for stability behavior of closed loop SP-PCL

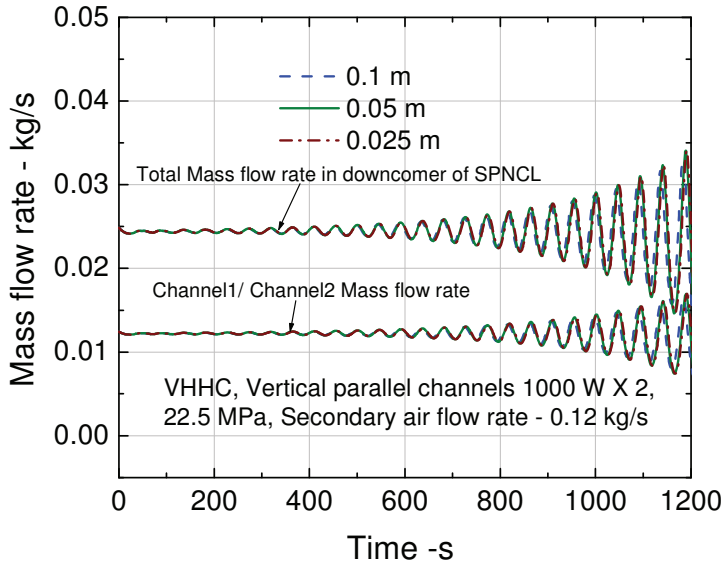

Figure 8: Grid size sensitivity study for stability behavior of closed loop SP-PCL

4.3.1.2 Effect of tolerance on pressure boundary condition

For closed loop natural circulation the pressure boundary condition to be satisfied at any time step is $\Sigma\Delta p = 0$. The solution is converged if $\left|\sum \Delta p\right| \leq tolernace\ value$. The stability predictions are found to be dependent on this tolerance value as shown in figure 9. Unrealistic oscillations are predicted for tolerance of 10 Pa, whereas similar oscillations are predicted for 1 Pa and 0.1 Pa. To save computational time pressure boundary condition tolerance of 1 Pa has been taken for further analysis.

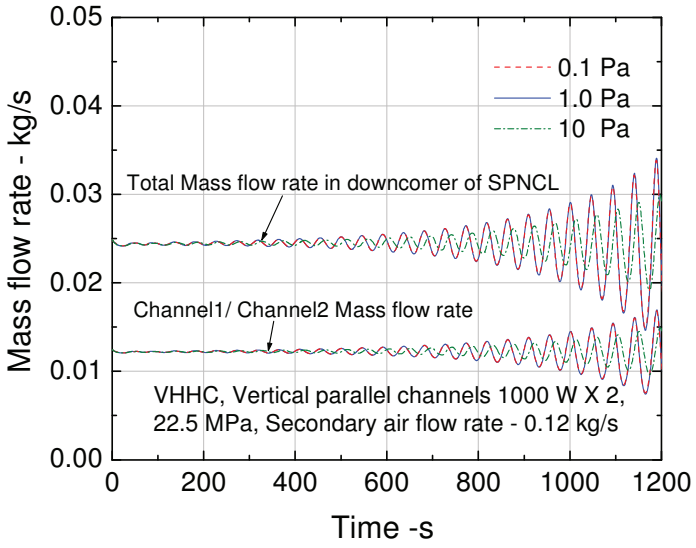

Figure 9: Effect of tolerance in Pressure boundary condition on stability behavior of closed loop SP-PCL

Considering above mentioned values of grid size, time step and pressure boundary condition convergence criterion a typical stable (100 W, 50 W in each channel), unstable (400 W, 200 W in each channel) and neutrally stable (200 W, 100 W in each channel) case was obtained at 22.5 MPa and 0.12 kg/s secondary air flow as shown in figure 10. The loop continues to be unstable at 6 kW (3 kW x 2), 8 kW (4 kW x 2), 10 kW (5 kW x 2) and 12 kW (6 kW x 2) as shown in figures 11 a & b, 12 a & b, 13 a & b and 14 a & b respectively. The instability is predicted for heater inlet temperature varying from 59 °C to 652 °C and no upper threshold of stability is observed as was observed for closed loop SPNCL with single heater channel for Horizontal Heater Horizontal Cooler, HHHC orientation (Sharma et al., 2014). However no instability is predicted for Vertical Heater Horizontal Cooler (VHHC) orientation of SPNCL for single heated channel without pipe wall thermal capacitance model as shown in figure 15 a & b.

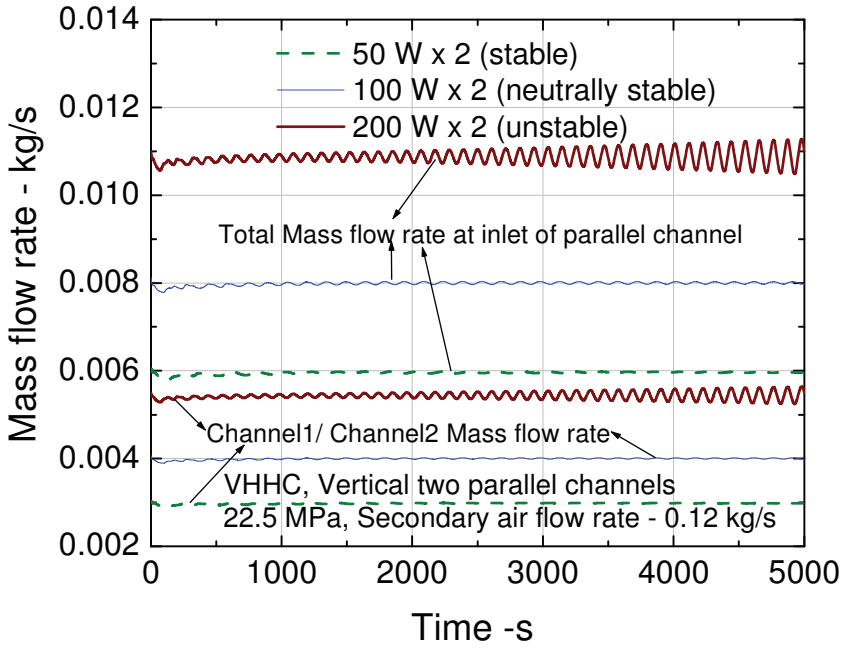

Figure 10: Stable, unstable and neutrally stable operating conditions for SP-PCL

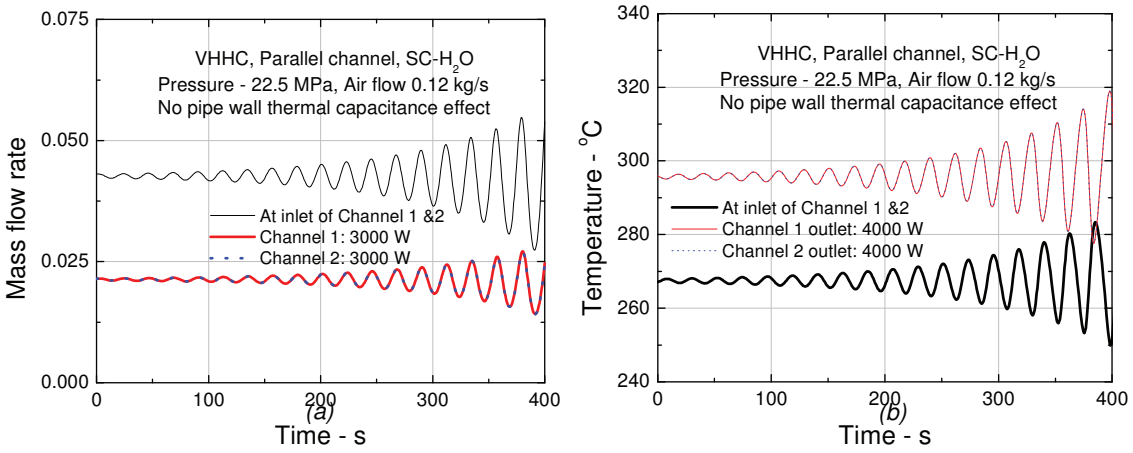

Figure 11: Stability predictions for closed loop SP-PCL at 6 kW total power.

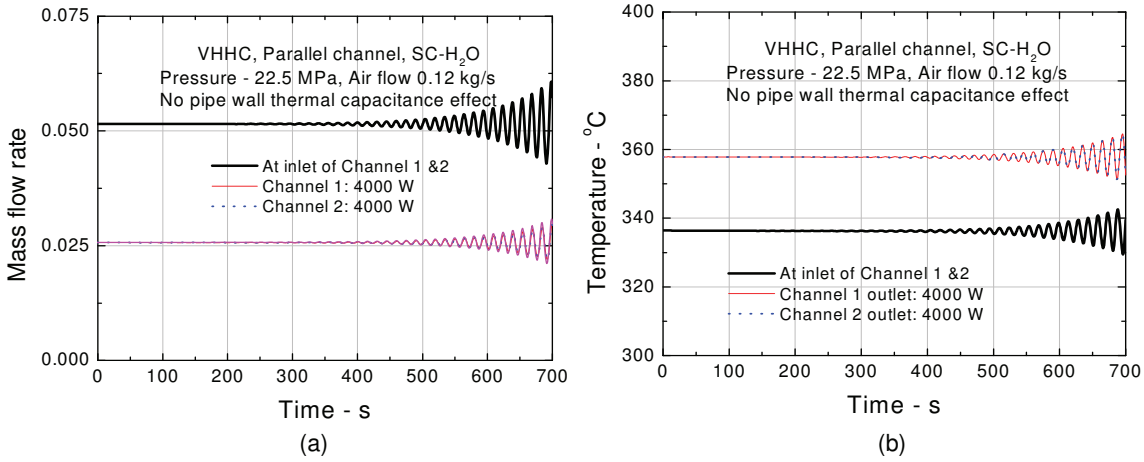

Figure 12: Stability predictions for closed loop SP-PCL at 8 kW total power.

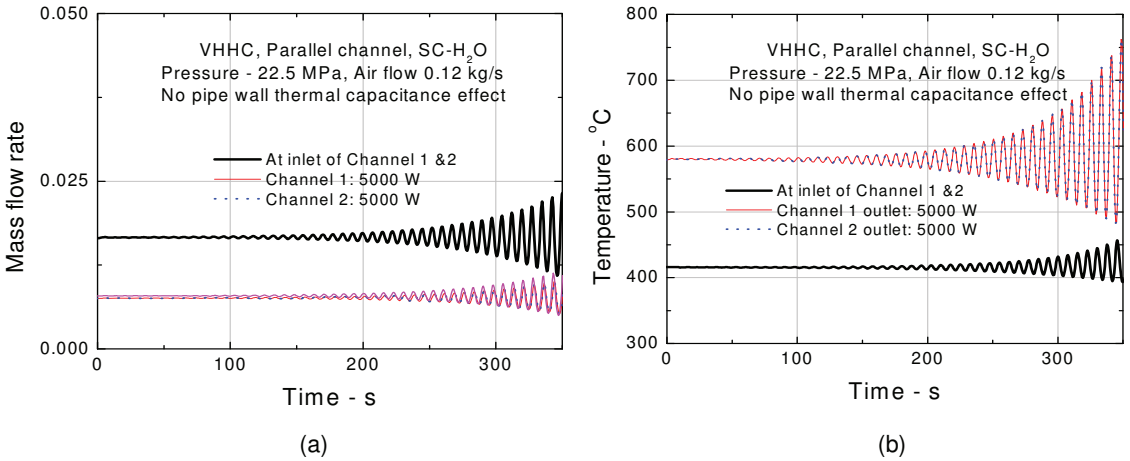

Figure 13: Stability predictions for closed loop SP-PCL at 10 kW total power.

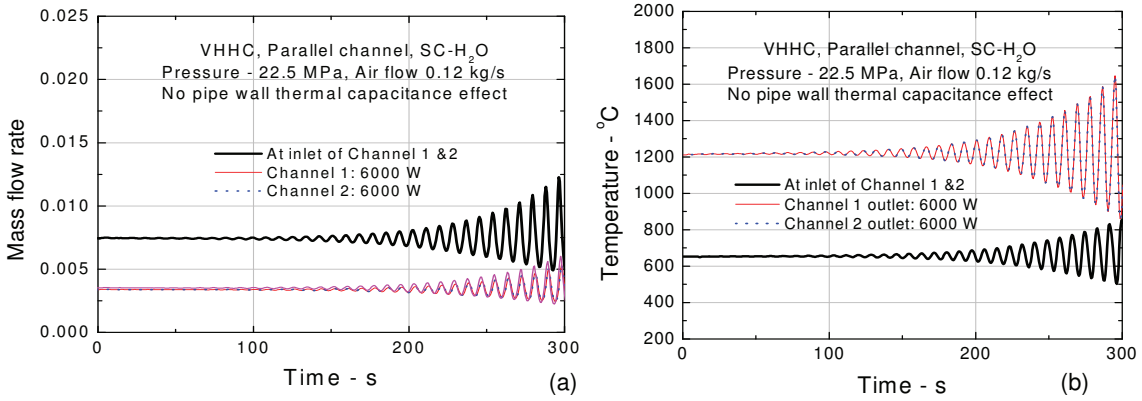

Figure 14: Stability predictions for closed loop SP-PCL at 12kW total power.

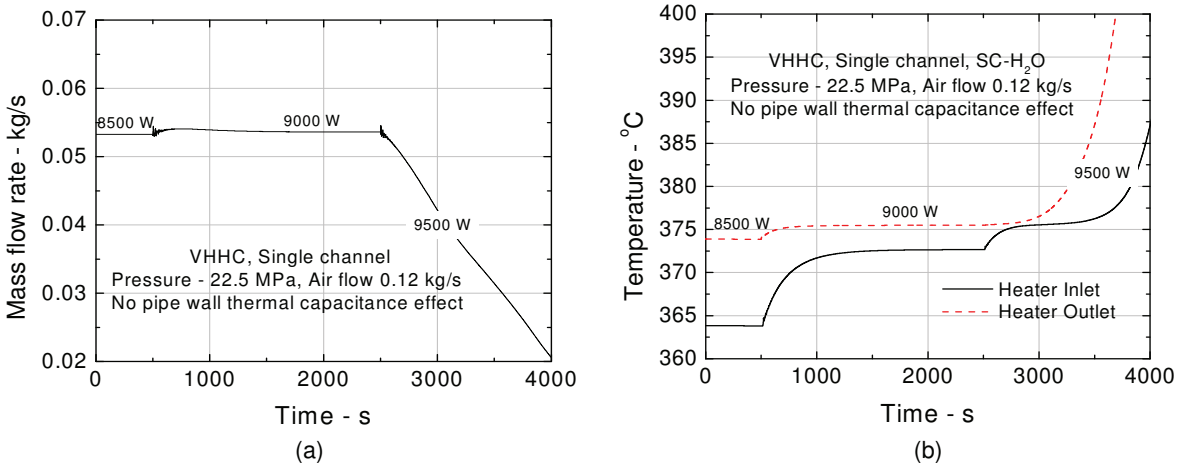

Figure 15: Stability predictions for closed loop SPNCL having single heated channel for VHHC orientation.

For same total power SP-PCL is more unstable for equal distribution of power in the two channels, however, for unequal power distribution in the two channels the loop stabilizes. For total power of 2000 W with 1000 W in each channel the SP-PCL is unstable as shown in figure 16. The loop is still unstable for unequal power distribution of 1300 W and 700 W in the two channels as shown in figure 17. However the loop becomes neutrally stable for distribution of 1500 W and 500 W in the two channels as shown in figure 18.

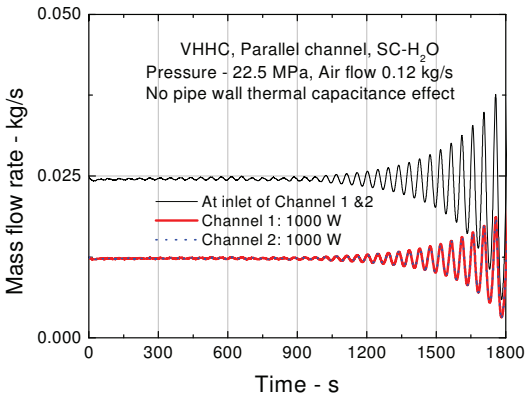

Figure 16: Unstable behavior of SP-PCL for equal distribution of power.

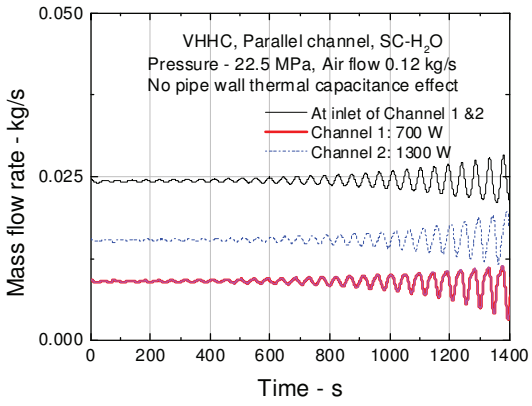

Figure 17: Unstable behavior of SP-PCL for unequal distribution of power.

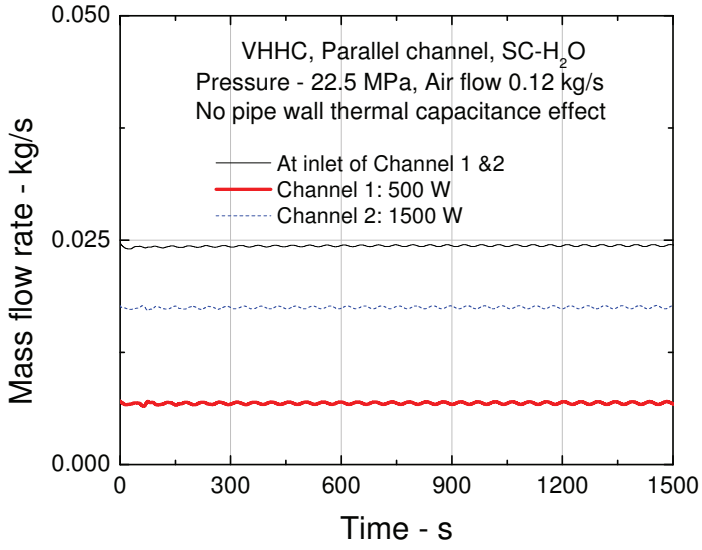

Figure 18: Neutrally stable behavior of SP-PCL for unequal distribution of power

6.1.3 Stability analysis with pipe wall thermal capacitance effect

One dimensional model for simulating thermal capacitance of pipe wall was incorporated in NOLSTA-p code based on the same methodology used in NOLSTA code (Sharma et al., 2013). The large instability zone as observed in the previous section (figures 11, 12, 13 & 14) vanishes by including pipe wall capacitance. The loop is stable even near the pseudo-critical temperature range as shown in figure 19 a & b.

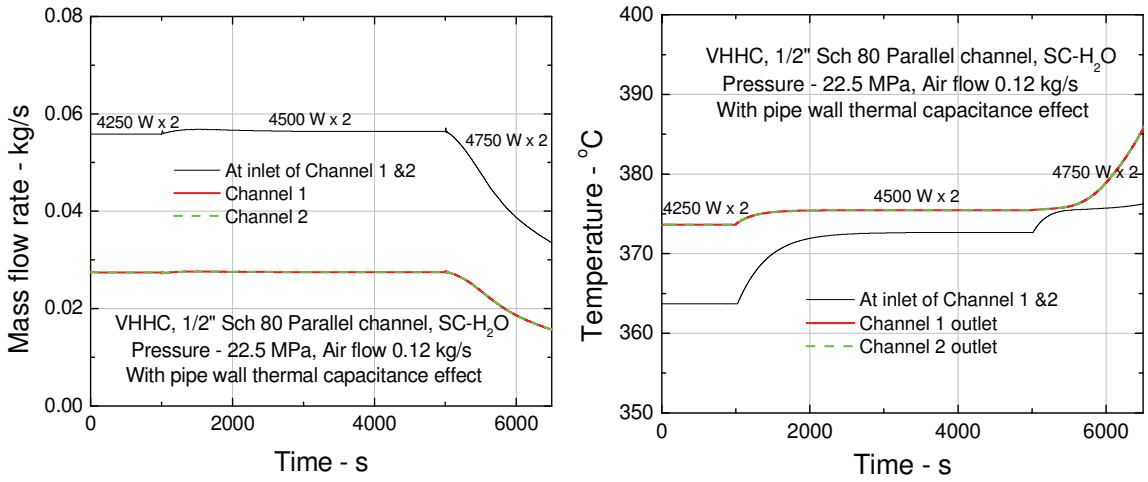

Figure 19: Stability predictions for ½" Sch.80 SP-PCL considering pipe wall thermal capacitance.

7. Conclusion

A computer code NOLSTA-p has been developed for steady state and stability analysis of supercritical pressure parallel channel loop. The code has been qualitatively assessed with experimental data reported by Xiong et al. (2012) with a maximum deviation of 9.4%. The steady state characteristic of SP-PCL is same as that of single channel SPNCL where the total mass flow rate first increases with increase of power due to increase of buoyancy head and then reduces due to increase of frictional resistance. The NOLSTA-p code predicts large unstable zone for SP-PCL (having two vertical parallel heaters and horizontal cooler) without considering pipe wall thermal capacitance effect. However, the Vertical Heater Horizontal Cooler (VHHC) orientation of single channel SPNCL is completely stable without considering pipe wall thermal capacitance effect. For same total power, SP-PCL is more unstable for equal distribution of powers in the two channels, however, for unequal power distribution in the two channels the loop stabilizes. On incorporating wall thermal capacitance model the SP-PCL is predicted to be completely stable.

NOMENCLATURE

A	Flow area (m^2)
A_h	Heat transfer area (m^2)
D	Hydraulic diameter (m)
f	Friction factor
g	Acceleration due to gravity (m/s^2)
i	Enthalpy (J/kg)
K	Local loss coefficient
p	Pressure (N/m^2)
q'''	Heat applied/unit volume of coolant (W/m^3)
Re	Reynolds number ($\rho uD/\mu$)
t	Time (s)
u	Velocity (m/s)
U	Overall heat transfer coefficient ($W/m^2/K$)
w	Mass flow rate (kg/s)
x	Axial distance (m)
z	Elevation (m)

Greek Symbols

ρ	Density (kg/m^3)
μ	Dynamic Viscosity (kg/m/s)
Φ	Inclination angle of the pipe with respect to vertical direction
Δ	an incremental change in a variable

Subscripts

c	Cooler
h	Heater
in,1	Inlet of channel-1
in,2	Inlet of channel-2
j	Current node
j+1	Next node
out,1	Outlet of channel-1
out,2	Outlet of channel-2

Superscripts

n	Current time step
n+1	Next time step

References

1. Adelt, M., Mikielewicz, J., 1981. Heat transfer in a channel at supercritical pressure, International Journal of Heat and Mass transfer, vol. 44., pp. 1667-1674.

2. Ambrosini, W., Sharabi, M., 2008. Dimensionless parameters in stability analysis of heated channels with fluids at supercritical pressures. Nuclear Engineering and Design 238, 1917–1929.

3. Bushby, S.J., Dimmick, G.R., Duffey, R.B., Spinks, N.J., Burrill, K.A., Chan, P.S.W., 2000. Conceptual designs for advanced high-temperature CANDU reactors, SCR-2000, Nov.6-8, Tokyo, paper 103.

4. Chatoorgoon, V., 2001. Stability of supercritical fluid flow in a single-channel natural-convection loop, International Journal of Heat and Mass Transfer 44, 1963-1972.

5. Chatoorgoon, V., Voodi, A., Upadhye, P., 2005. The stability boundary for supercritical flow in natural-convection loops Part II: CO2 and H2, Nuclear Engineering and Design 235, 2581–2593.

6. Chen, L., Zhang, X.R., Yamaguchi, H., Liu, Z. S., 2010. Effect of heat transfer on instabilities and transitions of supercritical CO2 flow in a natural circulation loop, International Journal of Heat and Mass Transfer 53, 4101-4111.

7. Dogan, T., Kakac, S., Veziroglu, T.N., 1983. Analysis of forced-convection boiling flow instabilities in a single- channel upflow system, Int. J. Heat and fluid flow 4, 145.

8. Harden, D., Boggs, J., 1964. Transient flow characteristics of a natural circulation loop operated in the critical region, Proc. Heat transf. Fluid mech. Inst., 38.

9. Hou, D., Lin, M., Liu, P., Yang, Y., 2011. Stability analysis of parallel-channel systems with forced flows under supercritical pressure, Annals of Nuclear Energy 38, 2386–2396.

10. Jain, R., Corrandini, M.L., 2006. A linear stability analysis for natural-circulation loops under supercritical conditions, Nuclear Technology, Vol. 155, 312-323.

11. Jain, P.K., Rizwan-uddin, 2008, Numerical analysis of supercritical flow instabilities in a natural circulation loop, Nuclear Engineering and Design 238, 1947-1957.

12. Lomperski, S., Cho, D., Jain, R., Corradini, M.L., 2004. Stability of a natural circulation loop with a fluid heated through the thermodynamic pseudo-critical point, Proceedings of ICAPP'04, Pittsburgh, PA USA, June 13-17, Paper 4268.

13. Sharma, M., Vijayan, P.K., Pilkhwal, D.S. and Asako, Y., 2013, Steady state and stability characteristics of Natural Circulation loops operating with carbon dioxide at supercritical pressures for open and closed loop boundary conditions, Nuclear Engineering and Design 265, 737–754.

14. Sharma, M., Vijayan, P.K., Pilkhwal, D.S. and Asako, Y., 2014, Natural convective flow and heat transfer studies for supercritical water in a rectangular circulation loop, Nuclear Engineering and Design 273, 304–320.

15. Silin, V.A., Voznesensky, V.A., Afrov, A.M., 1993, The light water integral reactor with natural circulation of the coolant at supercritical pressure B: 500 SKDI, Nuclear Engineering and Design 144, 327-336.

16. Su, Y., Feng, J., Zhao, H., Tian, W., Su, G., Qiu, S., 2013, Theoretical study on the flow instability of supercritical water in the parallel channels, Progress in Nuclear Energy 68, 169 - 176

17. T'Joen, C., Rohde, M., 2012. Experimental study of the coupled thermo-hydraulic–neutronic stability of a natural circulation HPLWR, Nuclear Engineering and Design 242, 221– 232.

18. Xiong, T., Yan, X., Xiao, Z., Li, Y., Huang, Y., Yu, J., 2012, Experimental study on flow instability in parallel channels with supercritical water, Annals of Nuclear Energy 48, 60–67.

19. Xi, X., Xiao, Z., Yan, X., Xiong, T., Huang, Y., 2014, Numerical simulation of the flow instability between two heated parallel channels with supercritical water, Annals of Nuclear Energy 64, 57–66

20. Yoshikawa, S., Smith Jr., R.L., Inomata, H., Matsumura, Y., Arai, K., 2005. Performance of a natural circulation system for supercritical fluids. Journal of Supercritical fluids 36, 70–80.